Raman study of intermultiplet crystal-field transitions in Sm_2CuO_4

T. Strach, T. Ruf, M. Cardona, and C. T. Lin
Max-Planck-Institut für Festkörperforschung, Heisenbergstrasse 1, 70569 Stuttgart, Germany

S. Jandl
Centre de Recherche en Physique du Solide, Département de Physique, Université de Sherbrooke, Sherbrooke, Québec, Canada J1K 2RI

V. Nekvasil
Institute of Physics, Czech Academy of Sciences, Cukrovarnická 10, 162 00, Prague 6, Czech Republic

D. I. Zhigunov, S. N. Barilo, and S. V. Shiryaev
Institute of Physics of Solids and Semiconductors, Ac. Sci. Belarus, Tolstoi street 4, 220072 Minsk, Belarus

(Received 8 December 1995)

Raman measurements were performed on single crystals of Sm_2CuO_4 in the temperature range from 300 to 10 K. We observe several Raman-active crystal-field (CF) transitions between the lowest level of the Sm^{3+} $^6H_{5/2}$ multiplet and other levels of the ^6H term. In contrast to CF excitations observed in the isostructural material Nd_2CuO_4, all peaks reported here are considerably broadened and show Lorentzian line shapes. We calculate the energies of the Sm^{3+} CF levels by using CF parameters obtained for Nd_2CuO_4 and find that they are in good agreement with the observed transitions. A least-squares fit of the CF parameters to the observed transition energies yields slightly improved parameters, which reproduce excellently the observed transitions. [S0163-1829(96)04429-3]

I. INTRODUCTION

Raman spectroscopy provides a powerful experimental method to observe rare-earth crystal-field (CF) transitions in many solids, including the electron-doped high-temperature superconductors $(R)_{2-x}Ce_xCuO_4$ (R=Nd, Pr or Sm) and their insulating parent compounds. While this has been demonstrated for Nd_2CuO_4,[1–3] $Nd_{1.85}Ce_{0.15}CuO_4$,[4] Pr_2CuO_4,[5,6] and $Pr_{1.85}Ce_{0.15}CuO_4$,[7] there are no reports so far on Raman-active CF transitions in Sm_2CuO_4. This system, however, is interesting for several reasons.

Like Nd^{3+}, Sm^{3+} is an ion with an odd number of electrons in its $4f$ shell. Placed inside a solid, the electric field of the surrounding ions lifts the degeneracy of the free ion $4f$ electronic states and leads to a new set of levels. All levels are at least twofold degenerate, as a consequence of Kramers' theorem.[8] A further lifting of the Kramers degeneracy is only possible by means of additional interactions, which break the time-reversal invariance of the rare-earth ion Hamiltonian, such as magnetic interactions with other atoms in the solid. In the case of Nd_2CuO_4, the Kramers degeneracy of the CF doublets is lifted due to magnetic interactions of the Nd sublattice with the antiferromagnetically ordered Cu sublattice. This has been clearly observed in Raman-scattering experiments,[2] and the ground-state splitting induced by magnetic interactions has been determined to be 3 ± 1 cm^{-1}. Similar interactions should also be observable with Raman spectroscopy in Sm_2CuO_4. It has been pointed out, however, that in Sm_2CuO_4 the magnetic moments of the Sm^{3+} ions align along the crystallographic z axis, perpendicular to the Cu magnetic moments, in contrast to Nd_2CuO_4, where both rare-earth and Cu magnetic moments align in the x-y plane, and that therefore the coupling between the Sm and Cu magnetic moments is completely frustrated.[9] If this is the case, one would expect the Kramers degeneracy of the doublets in Sm_2CuO_4 not to be destroyed by the Sm-Cu interaction.

Another reason to perform Raman spectroscopy of Sm_2CuO_4 CF transitions is the fact that Sm, in its natural isotopic abundance, is a very strong neutron absorber. This makes inelastic neutron-scattering (INS) spectroscopy only possible for Sm isotope-enriched samples, and up to now very few INS studies have been reported for ^{154}Sm-based high-T_c compounds,[9–11] in contrast to most other rare earths.[12–16] Additionally, usually only CF transitions within the lowest J-multiplet are detected in INS studies, while observations of intermultiplet transitions are scarce.[11,17] The small number of CF transitions detected by INS makes fits to theoretical models difficult: for a rare-earth ion on a crystal site of tetragonal symmetry there are five nonzero CF parameters of second, fourth, and sixth order, which have to be determined from the experimental data. Frequently, INS does not provide enough data for a sufficient overdetermination of the corresponding least-squares problem. The observation of more CF transitions by other means than INS is therefore highly desirable.

Finally, the study of CF levels in Sm_2CuO_4 also serves as an important check for CF parameters obtained from measurements in other materials with T' structure,[18] such as Nd_2CuO_4. It has been pointed out[19] that the variation of CF parameters across the lanthanide series is in general quite smooth. A good agreement between the two sets of CF parameters in Sm_2CuO_4 and Nd_2CuO_4 would thus further support the validity of both sets.

II. EXPERIMENT

Two Sm_2CuO_4 single crystals from different laboratories were used in this study. They will subsequently be called sample (A) and (B) for clarification. Sample (A) was grown from favorable CuO flux compositions in a platinum crucible.[20] The crystal was isolated from the flux by tipping the crucible over while the growth completed at 1110 °C. The as-grown crystal shows a shiny surface with tetragonal morphology and has a size of $4\times2\times0.5$ mm. Sample (B) is a $4\times3\times0.4$ mm piece, which was cut from a larger single crystal and subsequently cleaved to obtain a mechanically untreated surface. Details of its preparation are published elsewhere.[21] While sample (A) contains Sm in its natural isotopic abundance (3% ^{144}Sm, 15% ^{147}Sm, 11% ^{148}Sm, 14% ^{149}Sm, 7% ^{150}Sm, 27% ^{152}Sm, 23% ^{154}Sm) with an average atomic mass of 150.36, sample (B) was prepared from isotopically pure ^{154}Sm (atomic mass 153.92).

Raman measurements were performed in a backscattering configuration using a spectrometer equipped with a charge-coupled device (CCD) multichannel detector. Various Ar- and Kr-laser lines were used as excitation sources to verify resonance effects and to distinguish between Raman and luminescence signals. The laser power was below 15 mW in all experiments and the beam was focused to a 50 μm spot on the samples. The polarization of the incoming light was chosen either along the crystallographic x or z axis. We did not use an analyzer for the backscattered light. However, the polarization-selective response of the spectrometer gratings assured that the recorded light was predominantly ($>65\%$ at 514.5 nm, $>80\%$ at 647.1 nm) z polarized.

The samples were located in a closed-cycle He refrigerator with an attached temperature controller for measurements in the temperature range from 10 to 300 K. Several spectral regions around 300, 1200, 2400, and 3700 cm^{-1} were studied in order to observe transitions from the CF ground state to other CF levels in the $^6H_{5/2}$ multiplet and to levels in higher ^6H_J multiplets with J=7/2, 9/2, and 11/2. The recording time per spectrum varied between 15 min and several hours.

III. RESULTS

In Fig. 1 Raman spectra taken on sample (A) at different temperatures in the energy range from 0 to 600 cm^{-1} are displayed. Clearly visible at all temperatures are three lines around 125, 225 and 510 cm^{-1}. The lines at 225 and 510 cm^{-1} have been observed at similar frequencies in all $(R)_2CuO_4$ materials of the T' structure[22,23] and are commonly attributed to the (R) A_{1g} and (O) E_g phonon vibrations, respectively. The line at 125 cm^{-1} is observed less frequently due to its weak Raman response, and its assignment to the (R) E_g phonon vibration is still somewhat controversial.[24] To our knowledge, it has not been reported in Sm_2CuO_4 before. The observation of excitations with E_g symmetry, which are Raman forbidden in zz scattering geometry is due to the missing analyzer as mentioned in the previous section. In addition to these lines a broader structure at 200 cm^{-1} develops at low temperatures, which is absent at 300 K and only visible as a shoulder of the strong A_{1g} peak at 40 K. As shown in the inset of Fig. 1, this structure can also be observed with a different laser excitation wavelength.

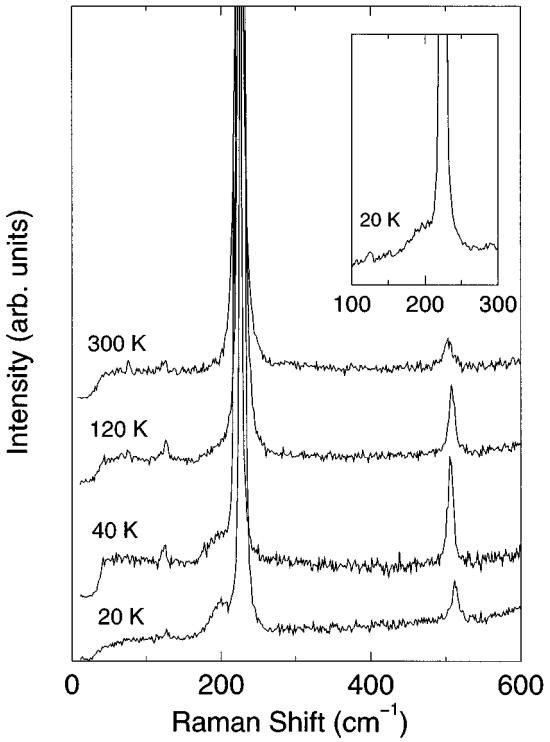

FIG. 1. Raman spectra of Sm_2CuO_4 at different temperatures in $y(zz)\overline{y}$ scattering configuration. The peaks at 125, 225, and 510 cm^{-1} correspond to phonons, the one at 200 cm^{-1} is a CF excitation. The laser wavelength for all spectra is 514.5 nm. Inset: spectrum around 200 cm^{-1} at 20 K observed with the 488.0 nm laser line.

A comparison between the Raman spectra of sample (A) and sample (B) at room temperature is displayed in Fig. 2 for zz and xz polarization configurations. While the line shapes are essentially the same in both samples, a careful determination of their position yields clearly observable shifts: In sample (A) the lines are located at 125.1($\pm$0.5) and 223.6($\pm$0.2) cm^{-1}, their position in sample (B) is at 123.0($\pm$0.3) and 220.7($\pm$0.2) cm^{-1}, as determined by Lorentzian fits. This results in a shift of 2.1($\pm$0.8) and 2.9($\pm$0.4) cm^{-1}, respectively. To exclude any errors due to a possible spectrometer drift, the position of the exciting laser line has been checked immediately before and after each of these measurements.

Figure 3 shows two Raman-active excitations around 1180 and 1380 cm^{-1} measured on sample (A) at different temperatures. In contrast to the shoulder at 200 cm^{-1}, these excitations remain observable at room temperature, however, their intensity is strongest at 20 K. Furthermore, the excitation around 1180 cm^{-1} clearly shows linewidth broadening and frequency softening with increasing temperature, shifting its position from 1183 cm^{-1} at 20 K to $\approx$ 1170 cm^{-1} at room temperature. The excitation around 1380 cm^{-1} shows a similar behavior. We have fitted the 1180 cm^{-1} line with a Lorentzian line shape and plot position and width vs temperature in Fig. 4. The frequency shift with increasing temperature seems somewhat more pronounced in sample (A), however, the position at 20 K as well as the widths at all

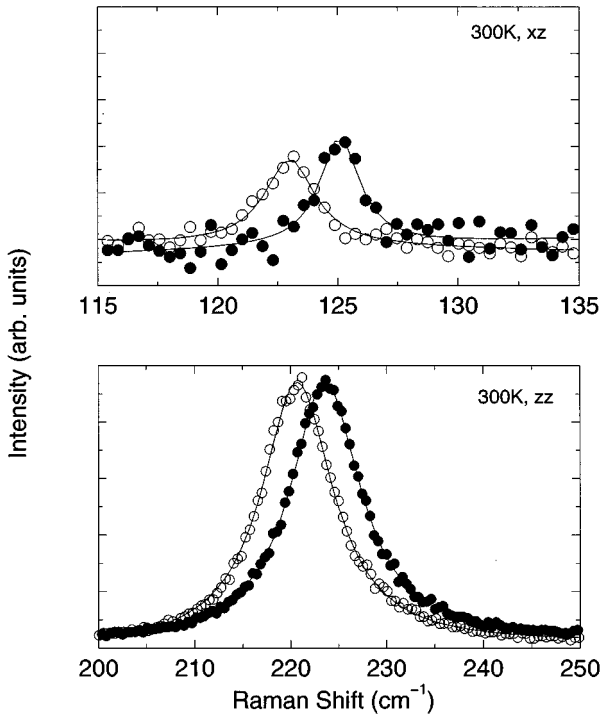

FIG. 2. Sm phonons at 300 K observed in zz and xz scattering configuration. Full symbols correspond to sample (A) (average Sm atomic mass 150.36), open symbols to sample (B) (average atomic mass 153.92). The solid lines correspond to Lorentzian profiles obtained from a least-squares fit to the experimental data.

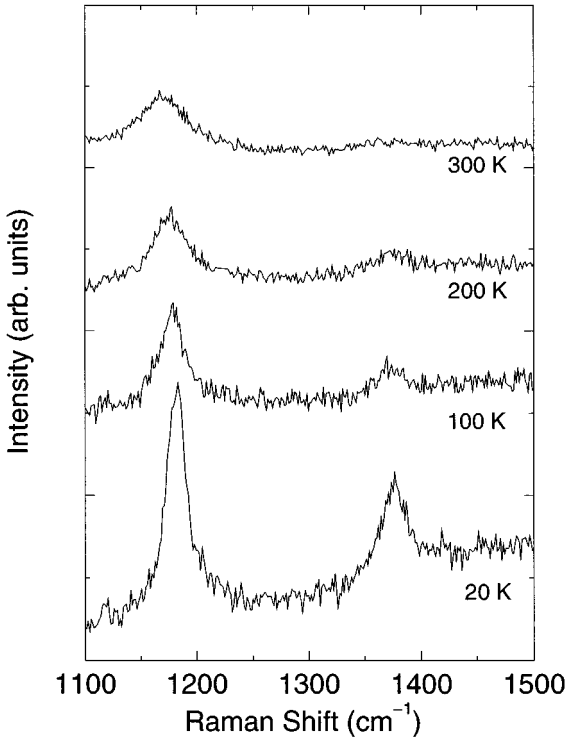

FIG. 3. $J=7/2$ CF excitations of Sm_2CuO_4 at different temperatures. All spectra were taken on sample (A) in $y(zz)\bar{y}$ scattering configuration with the 514.5 nm laser line as excitation source.

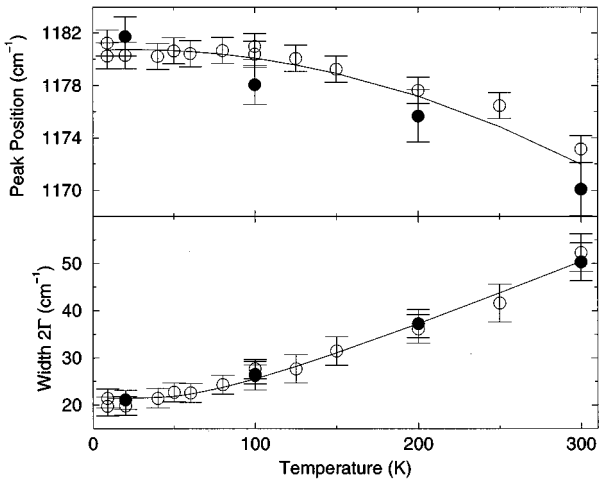

FIG. 4. Temperature evolution of the center frequency and Lorentzian width 2Γ (full width at half maximum) of the CF transition observed around 1180 cm^{-1}. Full symbols correspond to sample (A), open symbols to sample (B). The solid line in the upper part of the figure serves as a guide to the eye. The solid line in the lower part of the figure is a fit to the experimental data as described in the text.

temperatures are identical in both samples. In all cases a single Lorentzian profile gives an accurate fit to the observed line shape and no sign for a doublet peak structure or a strong line asymmetry can be detected.

Finally, Fig. 5 shows further excitations observed at 10 K in sample (B) at 2369, 2567, 3760, and 3896 cm^{-1}. All of them have been observed with different laser excitation lines, in order to ensure that they are Raman lines and not luminescence.

IV. DISCUSSION

A. Rare-earth phonons

While an isotopically pure $^{154}Sm_2CuO_4$ single crystal is not necessary for the observation of Raman-active CF transitions, it is very helpful to identify Sm-related phonons by their isotope shift: a crystal phonon mode with frequency ω, which is entirely due to a sublattice vibration of ions of mass m will shift to a new frequency ω' when these ions are replaced by a different isotope of mass m'. In a simple harmonic model, the relative frequency shift is given by

$$\frac{\Delta\omega}{\omega}=1-\frac{\omega'}{\omega}=1-\sqrt{\frac{m}{m'}},$$

where $\Delta\omega=\omega-\omega'$ is the absolute frequency shift of the vibration. Comparing sample (A) with an average atomic Sm mass of 150.36 and sample (B) containing pure ^{154}Sm (isotopic mass 153.92) one expects a relative frequency shift of -1.18% for pure Sm vibrations. From the Lorentzian fits to the lines in Fig. 2 one obtains relative frequency shifts of $-1.3(\pm0.2)\%$ and $-1.7(\pm0.6)\%$, respectively, for the 223

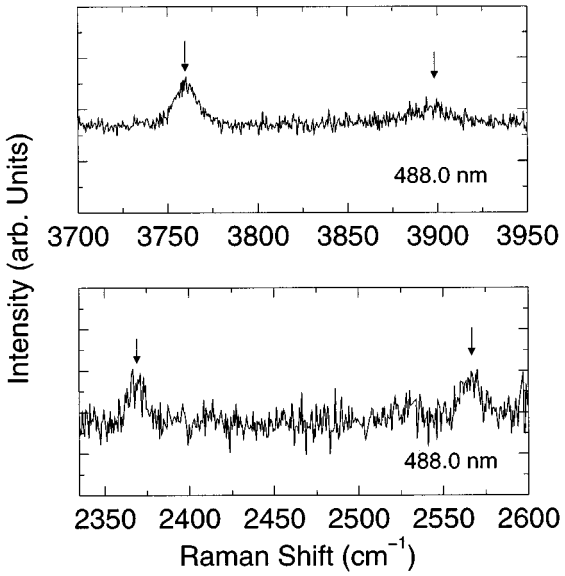

FIG. 5. Higher CF excitations observed in sample (B) in $y(zz)\bar{y}$ scattering configuration.

and 125 cm^{-1} lines. This conclusively proves that both excitations are Raman-active phonons which involve mainly Sm vibrations and that the 125 cm^{-1} line is indeed the Sm E_g mode.

B. Crystal-field excitations

Sm^{3+} has five electrons in its $4f$ shell. According to Hund's rules, the resulting free ion electronic ground state is $^6H_{5/2}$, a sixfold degenerate level with total angular momentum of $J=5/2$. Next in energy are the higher multiplets of the ^6H_J term with $J=7/2$, $J=9/2$, and $J=11/2$, which are eight-, ten-, and 12-fold degenerate, respectively. The energy difference due to spin-orbit coupling between these multiplets is only around 1000 cm^{-1} (Ref. 25), so that stronger J mixing is expected than for example in Nd_2CuO_4, where the separation between different ^4I_J multiplets is almost 2000 cm^{-1}. Additionally, for the higher Sm ^6H_J multiplets one also has to consider strong admixture of levels of the ^6F term.

In Sm_2CuO_4, the Sm^{3+} ions are located on sites with C_{4v} symmetry. Group theory predicts that the crystalline electric field splits the $^6H_{5/2}$ ground-state multiplet into one Γ_6 and two Γ_7 doublets, whereas the higher ^6H_J multiplets are split into $2\Gamma_6+2\Gamma_7$ ($^6H_{7/2}$), $3\Gamma_6+2\Gamma_7$ ($^6H_{9/2}$), and $3\Gamma_6+3\Gamma_7$ ($^6H_{11/2}$) doublets, respectively. The symmetry of excitations between these $4f$ states, which involves the direct product of their irreducible representations, corresponds to either

$$\Gamma_6\times\Gamma_6=\Gamma_7\times\Gamma_7=A_1+A_2+E$$

or

$$\Gamma_6\times\Gamma_7=\Gamma_7\times\Gamma_6=B_1+B_2+E.$$

The excitations of A_1, B_1, B_2, and E symmetry are Raman allowed.[26] In Nd_2CuO_4 it has been found that by far the strongest Raman-scattering efficiency occurs for the A_1 (zz) representation.[1] At low temperatures, where all rare-earth ions are in the CF ground-state configuration, one therefore expects to see only transitions to CF levels of the same symmetry as the CF ground state.

For a preliminary calculation of the energies and symmetries of the Sm^{3+} CF levels we used Nd^{3+} CF parameters obtained from Raman measurements on a Nd_2CuO_4 single crystal.[3] With these CF parameters we diagonalized the CF Hamiltonian in the subspace of the 12 lowest ^6H_J and ^6F_J multiplets. The resulting doublet symmetries and energies are listed in Table I. By comparing the calculated energies to the observed Raman excitations one notices that this first approximation already gives reasonable predictions for all detected lines and that indeed all features observed (besides the phonons of the T' structure) can be explained as CF transitions from the Γ_7 ground-state doublet to other Γ_7 doublets. In a next step, the five nonzero CF parameters up to sixth order allowed in tetragonal symmetry were used as free variables in a least-squares fit of the CF Hamiltonian to the experimentally observed transition energies. Intermediate-coupling wave functions and multiplet energies for the Sm^{3+} free ion were taken from the literature.[27,28] The mutliplet energies were kept constant during the fit. The fitted energies are listed in Table I; the agreement between theory and experiment is now found to be excellent for all transitions. The fitted Sm^{3+} as well as the Nd^{3+} CF parameters are given in Table II. We also want to point out that our calculated CF parameters are in good agreement with thermal expansion[29] and specific-heat measurements.[30]

While the strongest Raman-active CF transition in Nd_2CuO_4 at 1995 cm^{-1} appears as a doublet of Gaussian lines[1] with both doublet splitting and linewidths at 10 K of the order of a few cm^{-1}, all CF transitions in Sm_2CuO_4 have Lorentzian profiles with a residual width 2Γ of approximately 20 cm^{-1} at 10 K and no indication of a splitting. Poor sample quality can be excluded as a reason for the broad linewidth of the CF transitions, since we examined two crystals from different laboratories, which both showed an excellent Raman response with sharp phonon lines and only very little background scattering. The apparent absence of a splitting is consistent with the proposed orthogonal spin orientations of the Cu and Sm sublattices,[9] so that the Kramers degeneracy of the Sm^{3+} CF levels is not lifted. The comparatively large residual width of the CF transitions as well as their temperature dependence is probably caused by nonradiative, phonon-assisted decay of the CF excitations into other CF states within the same multiplet.[31] For the $^6H_{7/2}$ multiplet, a decay from the 1181 cm^{-1} Γ_7 level to the 1039 cm^{-1} Γ_6 level and from the 1375 cm^{-1} Γ_7 level to any of the lower levels (Γ_6 at 1313 and 1039 cm^{-1} and Γ_7 at 1181 cm^{-1}) is possible at zero temperature by emission of a phonon of the appropriate energy. Measurements of the phonon density of states in $(R)_2CuO_4$ (Ref. 32) and $YBa_2Cu_3O_7$ (Ref. 33) confirm that a sufficient number of phonons is present in these materials in the energy range between roughly 100 and 250 cm^{-1} to assist the nonradiative CF decays. The situation is different in Nd_2CuO_4: the CF level at 1995 cm^{-1} is very close in energy to the lowest level of the $^4I_{11/2}$ multiplet (1986 cm^{-1}),[3] so that only a very small number of *acoustic* phonons has the appropriate energy to assist a transition. Thus the 1995 cm^{-1} CF line in

TABLE I. Sm^{3+} CF levels in Sm_2CuO_4 observed experimentally, calculated from Nd^{3+} CF parameters (Ref. 3) and calculated using best-fit Sm^{3+} CF parameters.

	Experiment	Theory using Nd^{3+} CF parameters (Ref. 3)		fitted	
Multiplet	Energy (cm^{-1})	Energy (cm^{-1})	Symmetry i (Γ_i)	Energy (cm^{-1})	Symmetry i (Γ_i)
	3896	3908	7	3895	7
		3878	6	3820	6
		3837	6	3799	6
$^6H_{11/2}$	3760	3809	7	3768	7
		3674	6	3660	6
		3555	7	3560	7
	2567	2575	7	2568	7
		2555	6	2522	6
$^6H_{9/2}$		2494	6	2445	6
	2369	2406	7	2365	7
		2262	6	2263	6
	1375	1383	7	1375	7
		1353	6	1313	6
$^6H_{7/2}$	1181	1240	7	1180	7
		1031	6	1039	6
	196	221	7	201	7
$^6H_{5/2}$		108	6	119	6
	0	0	7	-1	7

Nd_2CuO_4 becomes much sharper at low temperatures than any of the CF levels detected in Sm_2CuO_4. In the case of Sm_2CuO_4, CF levels are located within 100 to 250 cm^{-1} below the levels considered. Thus the electrons can easily decay with the emission of an optical phonon.

We have fitted the temperature evolution of the linewidth of the 1181 cm^{-1} CF excitation to a model which allows for phonon-assisted, nonradiative decay to other CF levels within the $^6H_{7/2}$ multiplet. To reduce the number of free parameters in the fit we combine the two CF levels at 1313 and 1375 cm^{-1} in one level with an average energy of 1350 cm^{-1}, i. e., 169 cm^{-1} above the 1181 cm^{-1} CF excitation. Considering processes of phonon *absorption* to this higher level and *emission* processes to the one which is located 142 cm^{-1} below as responsible for the CF excitation linewidth the fitted function becomes

$$2\Gamma(T)=a_0\times[1+p(142\ \mathrm{cm}^{-1},T)]+a_1\times p(169\ \mathrm{cm}^{-1},T),$$

TABLE II. Sm^{3+} CF parameters (Wybourne notation) (Ref. 42) obtained by fitting the observed CF transitions as compared to Nd^{3+} CF parameters from Ref. 3.

Parameter	Sm^{3+} (cm^{-1})	Nd^{3+} (cm^{-1})
B_{20}	-329	-327(24)
B_{40}	-1524	-2264(45)
B_{44}	1662	1649(24)
B_{60}	239	215(17)
B_{64}	1345	1477(21)

where a_0 and a_1 represent coupling constants, and $p(\omega,T)$ is the Bose-Einstein statistical factor for a phonon of energy ω at temperature T.[26,31] As shown in Fig. 4, the experimentally observed behavior is excellently described by this model for values of $a_0=21.5$ cm^{-1} and $a_1=8.5$ cm^{-1}.

We were not able to detect Γ_6 to Γ_6 CF transitions at any temperature up to 300 K from the doublet at 100 cm^{-1} to higher doublets. This is in contrast to results obtained on Nd_2CuO_4, where transitions from the thermally populated Γ_7 doublet at 120 cm^{-1} to higher Γ_7 doublets are clearly observed at temperatures above 80 K.[1] Also, no direct Γ_7 to Γ_6 transitions could be detected. The reason, why the Raman activities of these transitions are so weak is not clear.

A point that deserves to be mentioned is the close proximity of the CF transition at $\approx$ 200 cm^{-1} to the Sm A_{1g} phonon at 223 cm^{-1}. Since both excitations have the same symmetry and similar energy, one might expect them to be coupled by the magnetoelastic interaction to form mixed excitations, each with partial phonon and CF character.[34] This has indeed been observed in $NdBa_2Cu_3O_{7-\delta}$ (Refs. 35 and 36) and $Pb_2Sr_2NdCu_3O_8$ (Ref. 37) where the coupling between the B_{1g} plane-oxygen phonon and a CF transition of the same symmetry leads to the formation of a double-peak structure at low temperature.

We have estimated the magnetoelastic interaction potential following the method described by Ruf *et al.*[38] The potential can be calculated by

$$V_{02}=\sum_{m,n}\frac{\partial B_n^m}{\partial Q}\times\langle\Psi_0|O_n^m|\Psi_2\rangle,$$

where Ψ_0 and Ψ_2 are the wave functions of the CF ground state and the Γ_7 state at 200 cm^{-1}, respectively, O_n^m are Stevens-operator equivalents,[39] B_n^m are the crystal-field parameters (in Stevens notation), and Q represents the phonon normal coordinate of the Sm A_{1g} phonon at 223 cm^{-1}. Since this model is based on the Stevens-operator technique, it does not include J mixing, and it is therefore sufficient to consider only the levels of the $^6H_{5/2}$ multiplet in the calculation. For a $J=5/2$ multiplet the sixth-order CF parameters B_6^m are zero in the Stevens model. Furthermore, since the A_{1g} vibration of the Sm atoms does not reduce the tetragonal symmetry of the crystal, the partial derivatives of the orthorhombic CF parameters B_2^2 and B_4^2 with respect to the phonon normal coordinate must also vanish. Thus one only has to consider the terms originating from the variation of the CF parameters B_2^0, B_4^0, and B_4^4 with phonon displacement. Our fitted Sm^{3+} CF parameters converted to Stevens notation[40] are $B_2^0 = -6.789\ cm^{-1}$, $B_4^0 = -0.4765\ cm^{-1}$, and $B_4^4 = 4.347\ cm^{-1}$. With these parameters we diagonalized the Stevens CF Hamiltonian in the subspace of the $^6H_{5/2}$ multiplet, which yields energy levels at 0, 145, and 318 cm^{-1}, somewhat larger than the results of the more sophisticated fit mentioned above. The wave functions of the two energy levels at 0 and 318 cm^{-1} are $\Psi_0 = 0.917|5/2,\pm 5/2\rangle - 0.400|5/2,\pm 3/2\rangle$ and $\Psi_2 = 0.400|5/2,\pm 5/2\rangle + 0.917|5/2,\pm 3/2\rangle$, respectively, close to the results from the fit, the main differences being due to additional admixtures of higher multiplets. For these wave functions the matrix elements of the Stevens operators become $\langle\Psi_0|O_2^0|\Psi_2\rangle = 5.499$, $\langle\Psi_0|O_4^0|\Psi_2\rangle = 87.98$ and $\langle\Psi_0|O_4^4|\Psi_2\rangle = 18.25$.

For the determination of the $\partial B_n^m/\partial Q$ we calculated the relative changes of the B_n^m with phonon displacement using a point-charge model.[41] Multiplying the result of this calculation with the Stevens CF parameters obtained from the fit yields values for $\partial B_n^m/\partial Q$ of -1.1596, -0.0049, and $-0.0735\ cm^{-1}$, for B_2^0, B_4^0, and B_4^4, respectively. Together with the previously determined matrix elements this results in an overall coupling potential of $-8.14\ cm^{-1}$. This is about 30% of the coupling potential calculated in $NdBa_2Cu_3O_7$ (Ref. 38) and, in the case of Sm_2CuO_4, results in a much weaker magnetoelastic coupling of electronic and phonon excitations.

As previously mentioned, the magneto-elastic coupling can cause the formation of a double peak. For the CF transition at about 200 cm^{-1}, using our spectra at 10 K, we determine exact center frequencies of 196 and 223 cm^{-1} and an intensity ratio of roughly 1:10 for the two peaks. If one assumes that the Raman activity of the lower excitation is entirely due to the phonon admixture one obtains from these numbers unrenormalized frequencies of 198.4 and 220.5 cm^{-1} as well as a coupling potential of $-7.8\ cm^{-1}$. This is in good agreement with the result of our theoretical estimation.

V. CONCLUSION

We have performed Raman-scattering experiments on two Sm_2CuO_4 single crystals differing in Sm isotopic composition in the temperature range from 300 to 10 K. The weak Raman line around 125 cm^{-1} was assigned to the Sm E_g phonon on the basis of its isotope shift. At low temperatures, we were able to detect seven crystal-field (CF) transitions between the CF ground-state doublet and higher CF levels of the $^6H_{5/2}$, $^6H_{7/2}$, $^6H_{9/2}$, and $^6H_{11/2}$ multiplets. All transitions have Lorentzian line shapes and similar widths of the order of 20 cm^{-1} at 10 K. A splitting of the Kramers-degenerate doublets, as seen for Nd_2CuO_4, was not detected. We obtained very accurate CF parameters by fitting the CF Hamiltonian to the observed CF level energies. The fitted parameters are similar in magnitude to the Nd^{3+} CF parameters obtained from the isostructural compound Nd_2CuO_4. We find a strong increase of the width of the 1180 cm^{-1} CF transition with increasing temperature which we attribute to phonon-assisted intramultiplet decay between CF levels.

ACKNOWLEDGMENTS

We thank H. Hirt and M. Siemers for technical assistance and T. Strohm for a careful reading of the manuscript. S.J. gratefully acknowledges the exchange program between the National Science and Engineering Research Council of Canada and the Deutsche Forschungsgemeinschaft, and V.N. the Grant Agency of the Czech Republic for its Grant No. 202/93/1165. Thanks are also due to P. Porcher for calculating the intermediate-coupling wave functions using parameters given in Ref. 27.

[1] S. Jandl, M. Iliev, C. Thomsen, T. Ruf, M. Cardona, B. M. Wanklyn, and C. Changkang, Solid State Commun. **87**, 609 (1993).
[2] P. Dufour, S. Jandl, C. Thomsen, M. Cardona, B. M. Wanklyn, and C. Changkang, Phys. Rev. B **51**, 1053 (1995).
[3] S. Jandl, P. Dufour, T. Strach, T. Ruf, M. Cardona, V. Nekvasil, C. Chen, and B. M. Wanklyn, Phys. Rev. B **52**, 15 558 (1995).
[4] S. Jandl, P. Dufour, T. Strach, T. Ruf, M. Cardona, V. Nekvasil, C. Chen, B. M. Wanklyn, and S. Piñol, Phys. Rev. B **53**, 8632 (1996).
[5] J. A. Sanjurjo, C. Rettori, S. Oseroff, and Z. Fisk, Phys. Rev. B **49**, 4391 (1994).
[6] M. L. Sanjuán, and M. A. Laguna, Phys. Rev. B **52**, 1 (1995).
[7] J. A. Sanjurjo, G. B. Martins, P. G. Pagliuso, E. Granado, I. Torriani, C. Rettori, S. Oseroff, and Z. Fisk, Phys. Rev. B **51**, 1185 (1995).
[8] H. A. Kramers, Proc. Amsterdam Acad. **33**, 959 (1930).
[9] A. G. Gukasov, V. A. Polyakov, I. A. Zobkalo, D. Petitgrand, P. Bourges, L. Boudarène, S. N. Barilo, and D. N. Zhigunov, Solid State Commun. **95**, 533 (1995).
[10] I. W. Sumarlin, S. Skanthakumar, J. W. Lynn, J. L. Peng, Z. Y. Li, W. Jiang, and R. L. Greene, Phys. Rev. Lett. **68**, 2228 (1992).
[11] M. Guillaume, H. Henggeler, A. Furrer, R. S. Eccleston, and V. Trounov, Phys. Rev. Lett. **74**, 3423 (1995).
[12] P. Allenspach, A. Furrer, R. Osborn, and A. D. Taylor, Z. Phys. B **85**, 301 (1991).

[13] U. Staub, J. Mesot, M. Guillaume, P. Allenspach, A. Furrer, H. Mutka, Z. Bowden, and A. Taylor, Phys. Rev. B **50**, 4068 (1994).
[14] A. T. Boothroyd, S. M. Doyle, D. M^{c}K. Paul, and R. Osborn, Phys. Rev. B **45**, 10 075 (1992).
[15] L. Soderholm, C.-K. Loong, and S. Kern, Phys. Rev. B **45**, 10 062 (1992).
[16] G. L. Goodman, C.-K. Loong, and L. Soderholm, J. Phys. Condens. Matter **3**, 49 (1991).
[17] U. Staub, L. Soderholm, R. Osborn, M. Guillaume, A. Furrer, and V. Trounov, J. Alloys Compounds **225**, 591 (1995).
[18] H. Shaked, P. M. Keane, J. C. Rodriguez, F. F. Owen, R. L. Hitterman, and J. D. Jorgensen, *Crystal Structures of the High-T_c Superconducting Copper-Oxides* (Elsevier, Amsterdam, 1994), p. 22.
[19] C. A. Morrison and R. P. Leavitt, in *Handbook of the Physics and Chemistry of Rare Earths*, edited by K. A. Gshneidner, Jr. and LeRoy Eyring (North-Holland, Amsterdam, 1982), p. 461.
[20] C. T. Lin (unpublished).
[21] S. N. Barilo and D. N. Zhigunov, Superconductivity: Phys. Chem. Technol. **2**, 138 (1989) (in Russian).
[22] Masayuki Udagawa, Yoshinori Nagaoka, Norio Ogita, Miki Masada, Jun Akimitsu, and Kohji Ohbayashi, Phys. Rev. B **49**, 585 (1994).
[23] M. A. Laguna, M. L. Sanjuán, A. Butera, M. Tovar, Z. Fisk, and P. Canfield, Phys. Rev. B **48**, 7565 (1993).
[24] M. L. Sanjuán, M. A. Laguna, S. Piñol, P. Canfield, and Z. Fisk, Phys. Rev. B **46**, 8683 (1992).
[25] K. N. R. Taylor and M. I. Darby, in *Physics of Rare Earth Solids* (Chapman and Hall, London, 1972).
[26] M. Cardona, in *Light Scattering in Solids II*, edited by M. Cardona and G. Güntherodt, Topics in Applied Physics, Vol. 50 (Springer, Berlin, 1982), p. 47.
[27] W. T. Carnall, H. Crosswhite, and H. M. Crosswhite (unpublished); W. T. Carnall, G. L. Goodman, K. Rajnak, and R. S. Rana (unpublished).
[28] C. A. Morrison and R. P. Leavitt, J. Chem. Phys. **71**, 2366 (1979).
[29] M. Diviš, V. Nekvasil, H. Müller, T. Holubar, C. Dusek, G. Schaudy, G. Hilscher, M. Vybornov, and P. Rogl, Solid State Commun. **90**, 257 (1994).
[30] T. Holubar, G. Schaudy, N. Pillmayr, G. Hilscher, M. Diviš, and V. Nekvasil, J. Magn. Magn. Mater. **104-107**, 479 (1992).
[31] S. Huefner, in *Optical Properties of Transparent Rare Earth Compounds* (Academic, New York, 1978), p. 119.
[32] I. W. Sumarlin, J. W. Lynn, D. A. Neumann, J. J. Rush, C. K. Loong, J. L. Peng, and Z. Y. Li, Phys. Rev. B **48**, 473 (1993).
[33] B. Renker, F. Gompf, E. Gering, D. Ewert, H. Rietschel, and A. Dianoux, Z. Phys. B **73**, 309 (1988).
[34] P. Thalmeier and P. Fulde, Phys. Rev. Lett. **49**, 1588 (1982).
[35] E. T. Heyen, R. Wegerer, and M. Cardona, Phys. Rev. Lett. **67**, 144 (1991).
[36] E. T. Heyen, R. Wegerer, E. Schönherr, and M. Cardona, Phys. Rev. B **44**, 10 195 (1991).
[37] R. Wegerer, C. Thomsen, T. Ruf, E. Schönherr, M. Cardona, M. Reedyk, J. S. Xue, J. E. Greedan, and A. Furrer, Phys. Rev. B **48**, 6413 (1993).
[38] T. Ruf, R. Wegerer, E. T. Heyen, M. Cardona, and A. Furrer, Solid State Commun. **85**, 297 (1993).
[39] K. W. H. Stevens, Proc. Phys. Soc. London Ser. A **65**, 209 (1952).
[40] A. J. Kassman, J. Chem. Phys. **53**, 4118 (1970).
[41] M. T. Hutchings, in *Solid State Physics: Advances in Research and Applications*, edited by Frederich Seitz and David Turnbull (Academic, New York, 1964), Vol. 16, p. 227.
[42] B. G. Wybourne, *Spectroscopic Properties of Rare Earths* (Interscience, New York, 1965).